Investigation of the ^{9}B nucleus and its cluster-nucleon correlations

Qing Zhao,[1,*] Zhongzhou Ren,[2,†] Mengjiao Lyu,[3,‡] Hisashi Horiuchi,[3,4] Yasuro Funaki,[5] Gerd Röpke,[6] Peter Schuck,[7,8] Akihiro Tohsaki,[3] Chang Xu,[1] Taiichi Yamada,[5] and Bo Zhou[9,10]

[1]*School of Physics and Key Laboratory of Modern Acoustics, Institute of Acoustics, Nanjing University, Nanjing 210093, China*
[2]*School of Physics Science and Engineering, Tongji University, Shanghai 200092, China*
[3]*Research Center for Nuclear Physics (RCNP), Osaka University, Osaka 567-0047, Japan*
[4]*International Institute for Advanced Studies, Kizugawa 619-0225, Japan*
[5]*Laboratory of Physics, Kanto Gakuin University, Yokohama 236-8501, Japan*
[6]*Institut für Physik, Universität Rostock, D-18051 Rostock, Germany*
[7]*Institut de Physique Nucléaire, Université Paris-Sud, IN2P3-CNRS, UMR 8608, F-91406, Orsay, France*
[8]*Laboratoire de Physique et Modélisation des Milieux Condensés, CNRS-UMR 5493, F-38042 Grenoble Cedex 9, France*
[9]*Institute for International Collaboration, Hokkaido University, Sapporo 060-0815, Japan*
[10]*Department of Physics, Hokkaido University, 060-0810 Sapporo, Japan*

(Received 22 January 2018; revised manuscript received 2 April 2018; published 22 May 2018)

In order to study the correlations between clusters and nucleons in light nuclei, we formulate a new superposed Tohsaki-Horiuchi-Schuck-Röpke (THSR) wave function which describes both spatially large spreading and cluster-correlated dynamics of valence nucleons. Using this new THSR wave function, the binding energy of ^{9}B is significantly improved in comparison with our previous studies. We calculate the excited states of ^{9}B and obtain an energy spectrum of ^{9}B which is consistent with the experimental results. This includes the prediction of the first $1/2^{+}$ excited state of ^{9}B which is not yet fixed experimentally. We study the proton dynamics in ^{9}B and find that the cluster-proton correlation plays an essential role for the proton dynamics in the ground state of ^{9}B. Furthermore, we discuss the density distribution of the valence proton with special attention to its tail structure. Finally, the resonance nature of excited states of ^{9}B is illustrated comparing root-mean-square radii between the ground and excited states.

DOI: 10.1103/PhysRevC.97.054323

I. INTRODUCTION

As one of the most important effects in nuclear physics, the cluster degrees of freedom have been extensively studied for various nuclear many-body problems [1–15], including the microscopic description of cluster states [14,15] and cluster radioactivity such as the α decay process [4,5]. With the discovery of α cluster condensation in light nuclei, the Tohsaki-Horiuchi-Schuck-Röpke (THSR) wave function has been proposed to describe gas-like cluster states in light nuclei, especially for ^{12}C and ^{16}O [8–15]. Investigations with the THSR wave function demonstrate the nonlocalized property of cluster dynamics in light nuclei such as ^{20}Ne [14]. In comparison with the generator coordinate method (GCM), which can be regarded as an advanced approach to the nuclear many-body problem, clustering states are found to be almost 100% accurately described by a single THSR wave function [14–18].

For the study of nonconjugate nuclei composed of both α clusters and valence nucleons, the THSR wave function has been successfully extended to the $^{9-11}$Be isotopes [11,19,20]. It is found that cluster-cluster correlations and nucleon-nucleon correlations can be well described by the THSR wave function in these systems [19,21]. However, there are still no studies devoted to the correlation between α clusters and valence nucleons. Since the cluster-nucleon correlation can be much different from the other two kinds of correlation, investigating the cluster-nucleon correlation can improve the understanding of the dynamics of valence nucleons in nonconjugate nuclei.

In order to study the dynamics of clusters and valence nucleons under the cluster-nucleon correlation, we provide a new form of the THSR wave function, and then, superpose THSR wave functions to describe both large spreading and cluster-correlated configurations for valence nucleons in light nuclei. This new superposed THSR wave function can be applied to most of nonconjugate nuclei like ^{9}Be, ^{9}B, ^{10}Be, etc. Here, we choose the nucleus ^{9}B, which has $\alpha + \alpha + p$ cluster structure, as the first application of our new framework, since there is a lack of good present understanding of the ^{9}B nucleus. Additionally, because of the extra Coulomb potential in comparison with its mirror nucleus ^{9}Be, the excited states with even parity in ^{9}B can be calculated with the THSR wave function more easily. We will discuss this case later with more detail.

By adding the cluster-nucleon correlation into the THSR wave function, we would like to see whether this extra correlation can improve the description of the ^{9}B nucleus with

*zhaoqing91@outlook.com
†Corresponding author: zren@tongji.edu.cn
‡mengjiao@rcnp.osaka-u.ac.jp

respect to the traditional THSR wave function. We are also interested in the different physical picture of the dynamics of valence nucleon which the cluster-nucleon correlations may bring. Furthermore, since the traditional THSR wave function has difficulties to describe the positive parity states of ^{9}Be and ^{9}B [11], we would like to try to produce the energy spectrum of ^{9}B as complete as possible, considering especially the first $1/2^+$ state in ^{9}B.

In Sec. II we formulate the superposed THSR wave function for ^{9}B. Then in Sec. III we show the results for the physical properties of ^{9}B and discuss the structure and dynamics of the cluster states, especially the cluster-nucleon correlation effect. Section IV contains the conclusions.

II. FORMULATION OF THSR WAVE FUNCTION OF ^{9}B

We first write the THSR wave function for ^{9}B in the form used in our previous publications [11]

$$\begin{aligned}&\Phi_0(\mathbf{r}_{i(i=1,2,\ldots 8)},\mathbf{r}_p)\\&=\prod_{i=1}^{2}\int d\mathbf{R}_i \exp\left(-\frac{R_{i,x}^2}{\beta_{\alpha,xy}^2}-\frac{R_{i,y}^2}{\beta_{\alpha,xy}^2}-\frac{R_{i,z}^2}{\beta_{\alpha,z}^2}\right)\\&\times\int d\mathbf{R}_p \exp\left(-\frac{R_{p,x}^2}{\beta_{p,xy}^2}-\frac{R_{p,y}^2}{\beta_{p,xy}^2}-\frac{R_{p,z}^2}{\beta_{p,z}^2}\right)\\&\times e^{im\phi_{\mathbf{R}_p}}\Phi^B(\mathbf{R}_1,\mathbf{R}_2,\mathbf{R}_p),\end{aligned}\tag{1}$$

where β_αs are Gaussian parameters for the nonlocalized motion of two α clusters and β_ps are Gaussian parameters for the valence proton. Here, we choose the direction of two α clusters as the z axis. The phase factor $e^{im\phi_{\mathbf{R}_p}}$ determines the intrinsic parity of the wave function [11]. $\phi_{\mathbf{R}_p}$ is the azimuthal angle of $\mathbf{R}_p$ in spherical coordinates. The parameter $m=1$ corresponds to the intrinsic negative parity while $m=0$ corresponds to the intrinsic positive parity. Φ^B is the Brink wave function which is written as

$$\begin{aligned}&\Phi^B(\mathbf{r}_{i=1,2,\ldots 8},\mathbf{r}_p,\mathbf{R}_1,\mathbf{R}_2,\mathbf{R}_p)\\&=\mathcal{A}\{\psi(\mathbf{r}_{k(k=1,2,3,4)},\mathbf{R}_1)\psi(\mathbf{r}_{l(l=5,6,7,8)},\mathbf{R}_2)\psi(\mathbf{r}_p,\mathbf{R}_p)\},\end{aligned}\tag{2}$$

where $\mathbf{R}_{(1,2)}$ and $\mathbf{R}_p$ are corresponding generator coordinates for the α clusters and valence proton, respectively. $\mathcal{A}$ is the antisymmetrization operator. $\psi(\mathbf{r}_{k(k=1,2,3,4)},\mathbf{R}_1)$, $\psi(\mathbf{r}_{l(l=5,6,7,8)},\mathbf{R}_2)$, and $\psi(\mathbf{r}_p,\mathbf{R}_p)$ are corresponding wave functions for the α clusters and valence proton, respectively. For each α cluster, four nucleons share one generator coordinate R.

To investigate correlations between the extra proton and each α cluster, we formulate the THSR wave function of ^{9}B as a superposition of both the cluster-correlated configuration and the large spreading configuration. It is denoted as the "superposed THSR wave function":

$$\Psi = c\Phi_1 + d\Phi_0.\tag{3}$$

Here, Φ_1 is the cluster-correlated configuration of ^{9}B, which describes the motion of the valence proton around the α cluster. Φ_0 corresponds to the large spreading configuration of ^{9}B in which the valence proton orbits around the ^{8}Be core. The coefficients c and d are the parameters of the superposed THSR wave function.

The THSR wave function in Eq. (1), which is denoted as "traditional THSR wave function", is used for Φ_0. The wave function corresponding to the correlation configuration Φ_1 is constructed in replacing the generator coordinate $\mathbf{R}_p$ of the valence proton in Φ_0 with coordinate $\mathbf{R}_p+\mathbf{R}_j$, as

$$\begin{aligned}&\Phi_{j(j=1,2)}(\mathbf{r}_{i(i=1,2,\ldots 8)},\mathbf{r}_p)\\&=\prod_{i=1}^{2}\int d\mathbf{R}_i \exp\left(-\frac{R_{i,x}^2}{\beta_{\alpha,xy}^2}-\frac{R_{i,y}^2}{\beta_{\alpha,xy}^2}-\frac{R_{i,z}^2}{\beta_{\alpha,z}^2}\right)\\&\times\int d\mathbf{R}_p \exp\left(-\frac{R_{p,x}^2}{\beta'^2_{p,xy}}-\frac{R_{p,y}^2}{\beta'^2_{p,xy}}-\frac{R_{p,z}^2}{\beta'^2_{p,z}}\right)\\&\times e^{im\phi_{\mathbf{R}_p+\mathbf{R}_j}}\Phi^B(\mathbf{R}_1,\mathbf{R}_2,\mathbf{R}_p+\mathbf{R}_j).\end{aligned}\tag{4}$$

The generator coordinate $\mathbf{R}_p$ is used to describe the correlated motion of the valence proton around the α cluster with generator coordinate $\mathbf{R}_j$, whose subscript j denotes one of the α clusters. Because of the antisymmetrization in Eq. (2), both functions Φ_1 and Φ_2 coincide. Therefore it is sufficient to take only Φ_1 in Eq. (3).

We also apply the angular-momentum projection technique $\hat{P}^J_{MK}|\Psi\rangle$ to restore the rotational symmetry [22],

$$\begin{aligned}|\Psi^{JM}\rangle &= \hat{P}^J_{MK}|\Psi\rangle\\&=\frac{2J+1}{8\pi^2}\int d\Omega D^{J*}_{MK}(\Omega)\hat{R}(\Omega)|\Psi\rangle,\end{aligned}\tag{5}$$

where J is the total angular momentum of ^{9}B.

The Hamiltonian of the ^{9}B nucleus can be written as

$$H=\sum_{i=1}^{9}T_i - T_{\text{c.m.}} + \sum_{i<j}^{9}V_{ij}^N + \sum_{i<j}^{9}V_{ij}^C + \sum_{i<j}^{9}V_{ij}^{ls}\tag{6}$$

with $T_{\text{c.m.}}$ the spurious kinetic energy of the center-of-mass motion. Volkov No. 2 [23] interaction is selected as the central force of the nucleon-nucleon potential

$$\begin{aligned}V_{ij}^N &= \left\{V_1 e^{-\alpha_1 r_{ij}^2} - V_2 e^{-\alpha_2 r_{ij}^2}\right\}\\&\times\{W - M\hat{P}_\sigma\hat{P}_\tau + B\hat{P}_\sigma - H\hat{P}_\tau\},\end{aligned}\tag{7}$$

where $M=0.6$, $W=0.4$, $B=H=0.125$, $V_1=-60.650$ MeV, $V_2=61.140$ MeV, $\alpha_1=0.309\,\text{fm}^{-2}$, and $\alpha_2=0.980\,\text{fm}^{-2}$.

The Gaussian soft core potential with three ranges (G3RS) [24] is taken as the spin-orbit interaction

$$V_{ij}^{ls} = V_0^{ls}\left\{e^{-\alpha_1 r_{ij}^2} - e^{-\alpha_2 r_{ij}^2}\right\}\mathbf{L}\cdot\mathbf{S}\hat{P}_{31},\tag{8}$$

where $\hat{P}_{31}$ projects the two-body system into triplet odd state. Parameters in V_{ij}^{ls} are taken as $V_0^{ls}=2000$ MeV, $\alpha_1=5.00\,\text{fm}^{-2}$, and $\alpha_2=2.778\,\text{fm}^{-2}$ from Ref. [25].

The Gaussian size parameter b for the nucleons in α clusters for ψ in Eq. (2) is set to $b=1.35$ fm, which is the same value as that used in our previous work in Ref. [11].

TABLE I. The $3/2^-$ rotational band of ^{9}B. $E^{\rm THSR}_{\rm old}$ denotes results obtained with the traditional THSR wave function Φ_0 used in our previous work. $E^{\rm THSR}_{\rm new}$ stands for the results obtained with our new superposed THSR wave function Ψ. $E^{\rm GCM}$ denotes results obtained with GCM calculation. Values in parentheses are corresponding excitation energies. Δ indicates the improvement obtained by our new superposed THSR wave function. All units of energies are in MeV.

State	$E^{\rm THSR}_{\rm old}$	$E^{\rm THSR}_{\rm new}$	Δ	$E^{\rm GCM}$	$E^{\rm exp}$ [26,27]
$7/2^-$(E.S.)	−47.0(6.9)	−48.3 (6.6)	1.3	−48.1(7.1)	−49.3 (7.0)
$5/2^-$(E.S.)	−51.4(2.5)	−52.4 (2.5)	1.0	−52.9(2.3)	−53.9 (2.4)
$3/2^-$(G.S.)	−53.9	−54.9	1.0	−55.2	−56.3

III. RESULTS AND DISCUSSIONS

Let us now discuss the energy spectrum of the ^{9}B nucleus obtained with the new superposed THSR wave function Ψ and compare it with the one obtained with the traditional THSR wave function Φ_0 used in our previous work [11]. This is shown in Table I. Both of these THSR wave functions Ψ and Φ_0 are variationally optimized. In this table, we also include the GCM results for the spectrum of ^{9}B, to justify the accuracy of the THSR wave functions.

From Table I we observe significant improvements for the binding energy of ^{9}B when using our new superposed THSR wave function. The new results are in much better agreements with the experimental values. Furthermore, we get almost the same results in comparison with the results from the GCM calculation in which 81 Brink basis states are superposed. This is a strong justification of our new wave function. The ground state rotational band of ^{9}B from the theoretical calculations and experiments are presented in Fig. 1. We take the energy minus the corresponding $\alpha+\alpha+p$ thresholds to set the thresholds as the origin of the y axis. Comparing with the traditional THSR wave function, the new superposed THSR wave function produces lower and denser energy levels, which is consistent with GCM and experiment

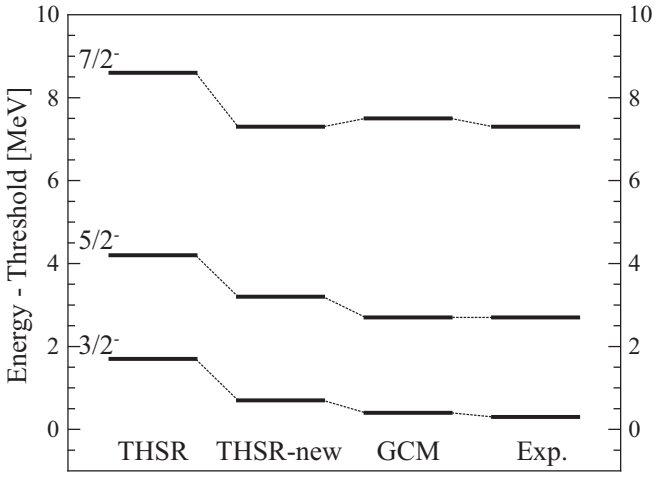

FIG. 1. Theoretical and experimental results of the energy spectrum of ^{9}B. The thresholds are set at the origin of the vertical axis.

TABLE II. Variationally optimized parameters and results for the ground state of ^{9}B. The first line denotes results with fixed $c=0$, the second line denotes results with variationally optimized $c=0.68$ and $d=0.32$, and the last line denotes results with fixed $d=0$. The remaining parameters are fixed to be the same as before. Units of β are in fm, and units of energies are in MeV.

c	d	$\beta_{\alpha,xy}$	$\beta_{\alpha,z}$	$\beta_{p,xy}$	$\beta_{p,z}$	$\beta'_{p,xy}$	$\beta'_{p,z}$	E
0	1.0	0.1	4.2	2.5	2.6	/	/	−53.9
0.68	0.32	0.1	5.5	5.9	3.1	0.5	2.5	−54.9
1.0	0	0.1	5.4	/	/	0.7	2.6	−52.3

results. The improvements obtained with the new THSR wave function indicate that the cluster-nucleon correlation can be a very important factor for describing nonconjugate nuclei. Since the GCM wave function can be seen as the optimal wave function for the physical system, the cluster-nucleon correlation may be the last effect left in the traditional THSR wave function for describing systems with α clusters and valence nuclei. If we take $\alpha+\alpha+p$ as the threshold, the threshold obtained from the THSR wave function is about −55.6 MeV, while the threshold from the experimental data is −56.6 MeV. This also indicates that the differences between our results and the experimental data are owing to the nucleon-nucleon interaction potential we choose (which gives the α binding energy 27.8 MeV instead of 28.3 MeV).

The values of the coefficients c and d reflect the contribution of each configuration. It is obvious that when the parameter $c=0$, the total wave function Ψ reduces to the traditional THSR wave function Φ_0. As already mentioned, it corresponds to a large spreading motion of the extra proton around the ^{8}Be core. When $d=0$, the total wave function Ψ reduces to Φ_1, which describes a strong correlation between the extra proton and the α cluster. It is convenient to discuss the traditional THSR wave function, the correlated THSR configuration and the new superposed THSR wave function by fixing the parameters c and

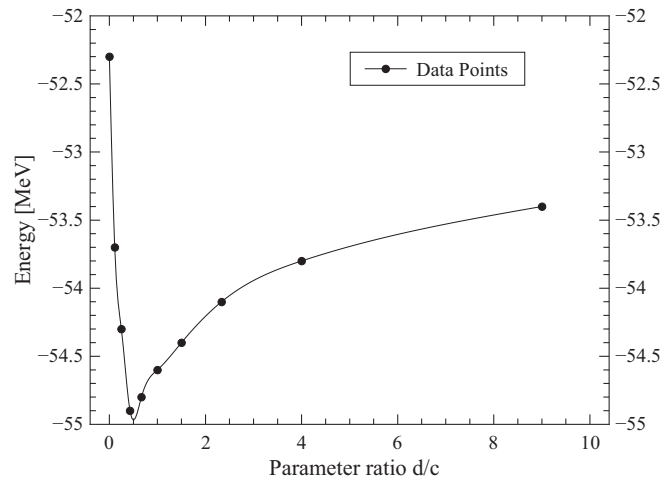

FIG. 2. Energy curve of the ground state of ^{9}B with respect to the ratio d/c, while other parameters are fixed to be the same as the optimized superposed THSR wave function.

TABLE III. rms radii for each state of ^{9}B obtained with the new superposed THSR wave function.

State	$3/2^-$	$5/2^-$	$7/2^-$	$1/2^-$	$1/2^+$	$3/2^+$
rms (fm)	2.81	2.87	3.00	3.04	4.05	4.16

d in the variational calculation. Since parameters c and d are not independent from each other, we optimized the ratio d/c by the variational calculation what corresponds to the coupling of these two different configurations. In Table II, we give the variationally optimized parameters and corresponding energies for the ground state of ^{9}B comparing with the other two extreme cases. The variationally optimized coefficients are shown in the second row of Table II as $c = 0.68$ and $d = 0.32$, with corresponding ratio $d/c = 0.47$. It is seen that the ground state energy of ^{9}B with optimized parameters is much lower than in the other two extreme cases. From the variational principle, we conclude that the coupling of two different configurations is energetically preferable and the new superposed THSR wave function provides a much better description than the traditional THSR wave function which corresponds to the $c = 0$ case. We also show the energy curve of the ground state of ^{9}B as a function of the ratio d/c in Fig. 2, in which the minimum point of the variational calculation can be seen clearly. Due to the almost equal values of the parameters $c/2$ and d, we can conclude that the cluster-correlated configuration and the large spreading configuration have both significant contributions to the dynamics of the ground state of ^{9}B. The difference in values of the parameter $\beta_{\alpha,z}$ between traditional and the new THSR wave function, shows that the distances between the two α clusters are also different in the two descriptions. The distance tends to be larger in spatial spreading when the cluster-nucleon correlation is taken into account.

We compare the density distributions of the valence proton obtained with the traditional and the new superposed THSR wave functions as shown in Fig. 3. It is clearly observed that the density distribution of the valence proton described by the new THSR wave function, is more compact in the x and y directions in comparison with the traditional one. This is because of the fact that in the new THSR wave function, correlation effects between the extra proton and α clusters, which are located near the z axis in the intrinsic frame, are taken into account.

To provide an explicit picture for the proton dynamics in ^{9}B, we also show the density distributions of the extra proton for the separate terms Φ_1 and Φ_0 of the total wave function Ψ, as shown in Fig. 4. We can see that the valence proton in the cluster-correlated configuration described by Φ_1 has a compact distribution as shown in the left panel (a), while the right panel (b) shows the remaining weak correlation effect between the ^{8}Be core and the valence nucleon as suggested by the much larger spread in space. We conclude that the inner region, which is close to the α clusters, mostly contributes with correlated configurations of the valence proton in Φ_1, while the outer region mostly contributes with the large spreading configuration of the valence proton described by Ψ_0. It should be noticed that, even though the extra proton is strongly correlated to each α cluster, this does not mean that the motion of the extra proton is localized, because the α clusters themselves are performing nonlocalized motion as discussed in Ref. [19].

To compare our new THSR wave function with the traditional one, we show the angular-averaged density distributions $\rho(R)$ of the valence proton in Fig. 5 in plotting $\ln[\rho(R)]$ as a function of R^2. For the traditional THSR function, the Gaussian behavior of the tail is clearly observed as shown by the dashed (blue) line. For the region $R < 3$ fm, the Gaussian behavior is modified because of the antisymmetrization with respect to the ^{8}Be core. The new THSR wave function deviates from the traditional one for the region $R > 4$ fm showing a longer tail, i.e., the density distribution spreads out compared with the Gaussian behavior. We conclude that the weakly bound valence proton in ^{9}B is not exactly described by a Gaussian, but has a long-range density tail. The new THSR wave function demonstrates the existence of such a long-range density tail.

We further apply the new superposed THSR wave function to the first $1/2^+$ excited state of ^{9}B. It is predicted in various theoretical models [25,28,29] that there might exist a $1/2^+$ excited state in ^{9}B. However, because this state is very broad,

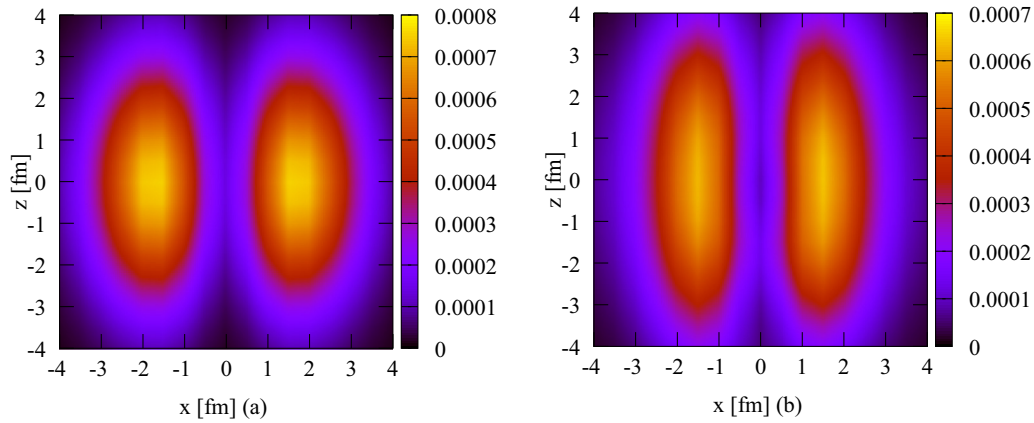

FIG. 3. Density distributions of the valence proton of ^{9}B in the $y = 0$ cross section obtained with different THSR wave functions. The left figure corresponds to traditional THSR wave function. The right one corresponds to the new THSR wave function. The unit of the density is fm^{-3}.

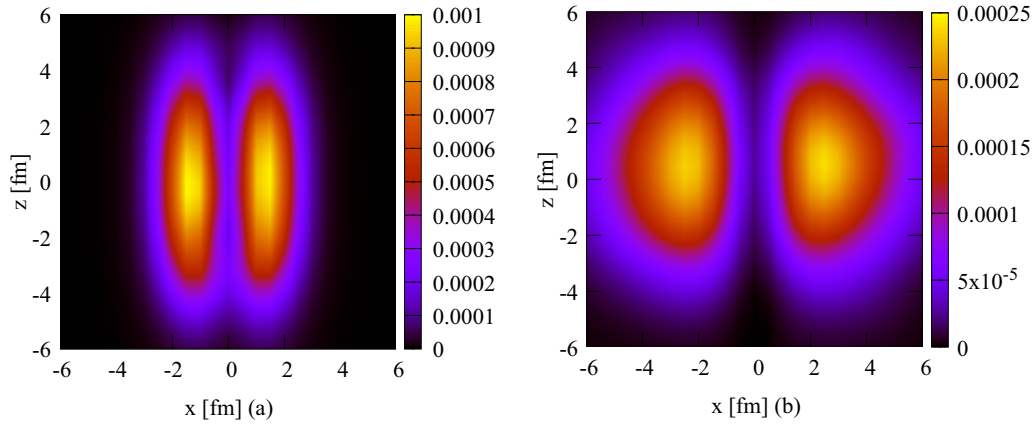

FIG. 4. Density distributions of the valence proton obtained with different terms in the new superposed THSR wave function. The left corresponds to the cluster-correlated term Φ_1. The right corresponds to the large spreading configuration Φ_0. Parameter βs are selected as the optimized values of the new superposed THSR wave function. The unit of the density is fm^{-3}.

the excited energy of this state is not yet fully confirmed by experiments [30–32]. We made some effort to calculate the $1/2^+$ state in ^{9}Be but failed. However, because of the Coulomb barrier in ^{9}B, we may have a chance to find a local energy minimum corresponding to the $1/2^+$ state in the ^{9}B nucleus. With our new THSR wave function, we indeed found such a local minimum from the variational calculation. Because of the limited computation power, we cannot confirm this minimum with high accuracy, but we observe that it continues to exists while we increase the precision, as shown in Fig. 6. Even though this local minimum is much shallower than the error bars, our results indicate that there might be an excited state of $1/2^+$ in ^{9}B with 1.7 MeV above the ground state. Comparing with many experimental results as shown in Fig. 7, our result of the first $1/2^+$ state of ^{9}B can fit the experiment value [26] very well.

Furthermore, we calculate the $3/2^+$ state, which belongs to the rotational band of the first $1/2^+$ state. The energy of this state is obtained as 4.2 MeV, which is consistent with the experimental value 4.3 MeV as predicted in Ref. [26]. This agreement further implies that the new superposed THSR wave function provides a good description for its band head, the $1/2^+$ state.

The root-mean-square (rms) radii are calculated for the each state of ^{9}B with the new THSR wave function as shown in Table III. For the $1/2^+$ rotational band of ^{9}B, the rms radii are much larger than the ones of the other states, because the decay of this state into the 0^+ ground state of ^{8}Be occurs via the s wave of the valence proton, and the decaying proton does not feel any centrifugal barrier. Hence the $1/2^+$ excited state is a resonance state which is spatially confined predominantly owing to the Coulomb barrier. This resonance nature is the main origin of the large radii of the $1/2^+$ state and its rotational band.

Furthermore, the computational efficiency of our variational calculation is seriously hampered by the broad distribution

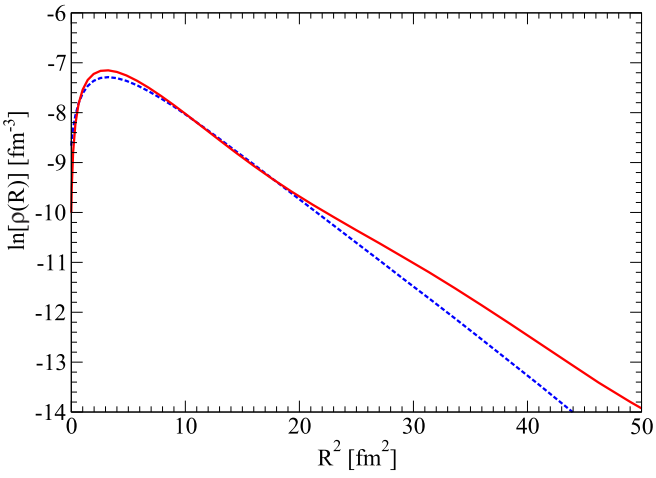

FIG. 5. The angular-averaged density distributions of the valence proton. The dashed (blue) line is obtained with the traditional THSR wave function while the full (red) line is obtained with the new THSR wave function.

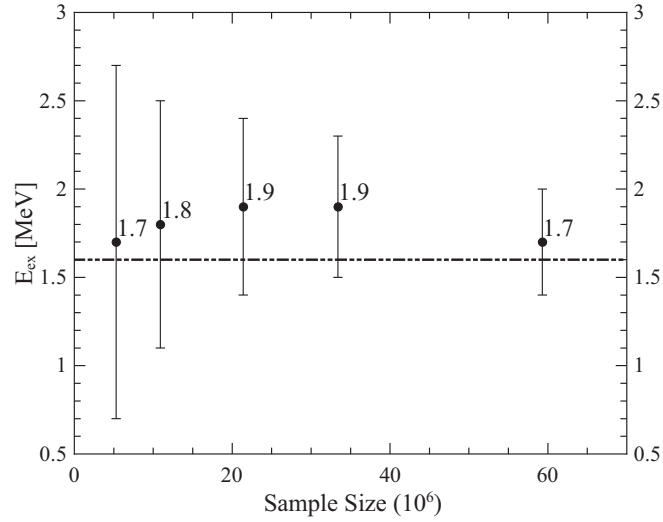

FIG. 6. The excitation energy of the $1/2^+$ state in ^{9}B with increasing sample size (10^6) in our Monte Carlo calculation. The dotted line denotes the experimental prediction in Ref. [26].

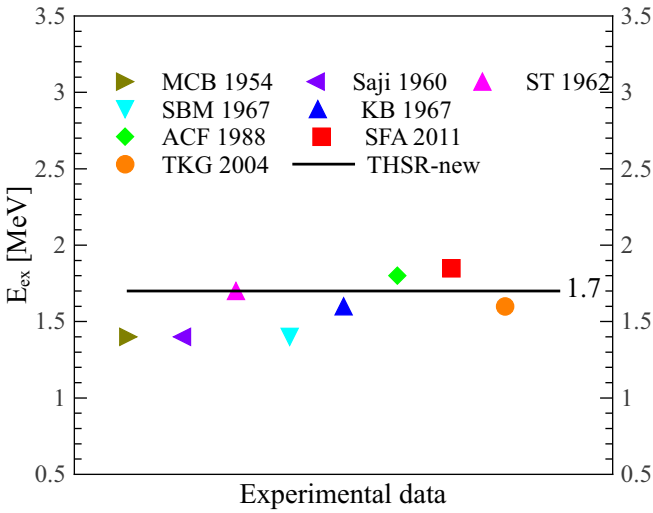

FIG. 7. The excited energy of the $1/2^+$ state of ^{9}B with our new superposed THSR wave function (line) compared with various experimental results (dots). The experimental results are from MCB 1954 [33], Saji 1960 [34], ST 1962 [35], SBM 1967 [36], KB 1967 [37], ACF 1988 [38], SFA 2011 [39], TKG 2004 [26].

of nucleons. For the calculation of the $5/2^+$ state of ^{9}B, the convergence cannot be obtained. This is the reason why we do not include the $5/2^+$ state result in the present work.

We present the total energy spectrum of ^{9}B obtained with the new superposed THSR wave function in Fig. 8. We observe systematic agreement between our theoretical results and the experimental values, which show the accuracy and efficiency of our new approach in describing general cluster states with coupling of α clusters and valence nucleons.

IV. CONCLUSION

We formulated a new superposed THSR wave function for nonconjugate nuclei with components corresponding to both the large spreading motion and the cluster-correlated motion for the valence nucleon and investigated the ^{9}B nucleus with the new wave function. The calculated energies of the $3/2^-$ rotational band are well improved in comparison with the previous version of the THSR wave function in Ref. [11], and much better agreement with the GCM results and the experimental values is obtained. Comparing the optimized wave function with each term of the superposition, it is shown clearly that both large spreading and cluster-correlated motion are essential for the description of the ^{9}B nucleus. The dynamics of valence proton and the cluster-proton correlation is further discussed in displaying density distributions of the valence proton. Results from variational calculation further suggest that there might be a $1/2^+$ excited state of ^{9}B at about 1.7 MeV which is consistent with experimental predictions. The rms radii of each state of

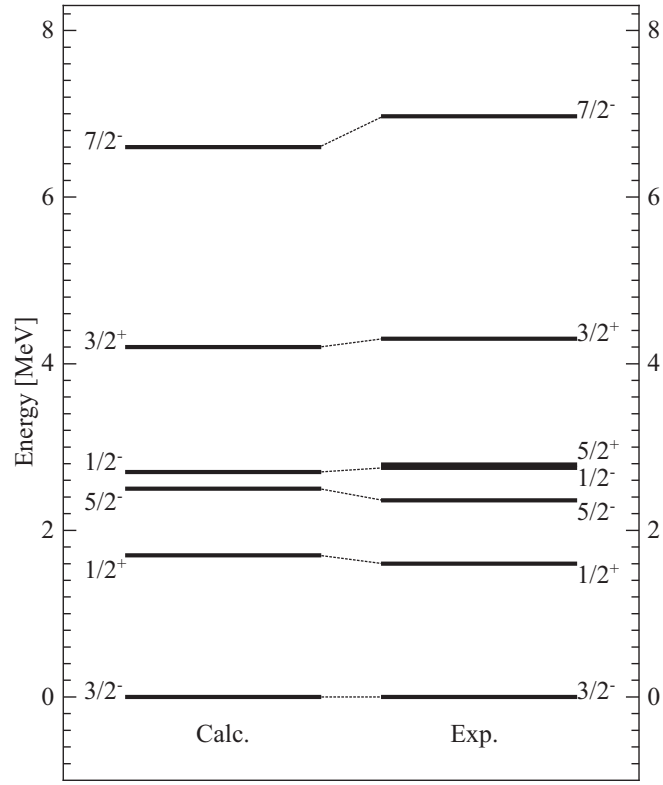

FIG. 8. Theoretical and experimental energy spectra of ^{9}B. The states with higher energy, which are found in experiment, are not considered in our calculation because of the limitation of computation power.

^{9}B are obtained and large spatial spreading is observed for the first $1/2^+$ excited state and its corresponding rotational band because of its resonance nature. Other states are also calculated with the new superposed THSR wave function, and we produce an energy spectrum of ^{9}B that agrees in a systematic way with the experimental values. This study further improves the understanding of both the physical property of ^{9}B nucleus and the cluster-nucleon correlations, which is beneficial for future extended investigations for neutron-rich or proton-rich nuclei going towards the nuclear drip line.

ACKNOWLEDGMENTS

The authors would like to thank Prof. Kimura and Prof. Kanada-En'yo for fruitful discussions. This work is supported by the National Natural Science Foundation of China (Grants No. 11535004, No. 11761161001, No. 11375086, No. 11120101005, No. 11175085, and No. 11235001), by the National Major State Basic Research and Development of China, Grant No. 2016YFE0129300, by the Science and Technology Development Fund of Macau under Grant No. 068/2011/A, and by the JSPS KAKENHI Grant No. JP16K05351.

[1] Y. Funaki, H. Horiuchi, and A. Tohsaki, Prog. Part. Nucl. Phys. **82**, 78 (2015).

[2] M. Freer, H. Horiuchi, Y. Kanada-En'yo, D. Lee, and U.-G. Meißner, arXiv:1705.06192.

[3] Y. Kanada-En'yo, H. Horiuchi, and A. Ono, Phys. Rev. C **52**, 628 (1995).
[4] C. Xu and Z. Ren, Phys. Rev. C **73**, 041301(R) (2006).
[5] Y. Ren and Z. Ren, Phys. Rev. C **85**, 044608 (2012).
[6] W. B. He, Y. G. Ma, X. G. Cao, X. Z. Cai, and G. Q. Zhang, Phys. Rev. Lett. **113**, 032506 (2014).
[7] Z. Yang, Y. Ye *et al.*, Phys. Rev. Lett. **112**, 162501 (2014).
[8] T. Yamada and P. Schuck, Eur. Phys. J. A **26**, 185 (2005).
[9] A. Tohsaki, H. Horiuchi, P. Schuck, and G. Röpke, Phys. Rev. Lett. **87**, 192501 (2001).
[10] Y. Funaki, H. Horiuchi, A. Tohsaki, P. Schuck, and G. Röpke, Prog. Theor. Phys. **108**, 297 (2002).
[11] M. Lyu, Z. Ren, B. Zhou, Y. Funaki, H. Horiuchi, G. Röpke, P. Schuck, A. Tohsaki, C. Xu, and T. Yamada, Phys. Rev. C **91**, 014313 (2015).
[12] B. Zhou, Y. Funaki, H. Horiuchi, Z. Ren, G. Röpke, P. Schuck, A. Tohsaki, C. Xu, and T. Yamada, Phys. Rev. C **89**, 034319 (2014).
[13] T. Suhara, Y. Funaki, B. Zhou, H. Horiuchi, and A. Tohsaki, Phys. Rev. Lett. **112**, 062501 (2014).
[14] B. Zhou, Y. Funaki, H. Horiuchi, Z. Ren, G. Röpke, P. Schuck, A. Tohsaki, C. Xu, and T. Yamada, Phys. Rev. Lett. **110**, 262501 (2013).
[15] B. Zhou, Z. Ren, C. Xu, Y. Funaki, T. Yamada, A. Tohsaki, H. Horiuchi, P. Schuck, and G. Röpke, Phys. Rev. C **86**, 014301 (2012).
[16] Y. Funaki, A. Tohsaki, H. Horiuchi, P. Schuck, and G. Röpke, Phys. Rev. C **67**, 051306(R) (2003).
[17] Y. Funaki, A. Tohsaki, H. Horiuchi, P. Schuck, and G. Röpke, Eur. Phys. J. A **24**, 321 (2005).
[18] Y. Funaki, H. Horiuchi, W. von Oertzen, G. Röpke, P. Schuck, A. Tohsaki, and T. Yamada, Phys. Rev. C **80**, 064326 (2009).
[19] M. Lyu, Z. Ren, B. Zhou, Y. Funaki, H. Horiuchi, G. Röpke, P. Schuck, A. Tohsaki, C. Xu, and T. Yamada, Phys. Rev. C **93**, 054308 (2016).
[20] M. Lyu, Z. Ren, H. Horiuchi, B. Zhou, Y. Funaki, G. Röpke, P. Schuck, A. Tohsaki, C. Xu, and T. Yamada, arXiv:1706.06538.
[21] Q. Zhao, Z. Ren, M. Lyu *et al.*, (unpublished) (2018).
[22] P. Ring and P. Schuck, *The Nuclear Many-Body Problem* (Springer-Verlag, New York, 1980), p. 474.
[23] A. B. Volkov, Nucl. Phys. **74**, 33 (1965).
[24] N. Yamaguchi, T. Kasahara, S. Nagata, and Y. Akaishi, Prog. Theor. Phys. **62**, 1018 (1979).
[25] S. Okabe and Y. Abe, Prog. Theor. Phys. **61**, 1049 (1979).
[26] D. R. Tilley, J. H. Kelley, J. L. Godwin, D. J. Millener, J. E. Purcell, C. G. Sheu, and H. R. Weller, Nucl. Phys. A **745**, 155 (2004).
[27] G. Audi, F. G. Kondev, M. Wang, B. Pfeiffer, X. Sun, J. Blachot, and M. MacCormick, Chin. Phys. C **36**, 1157 (2012).
[28] F. C. Barker, Phys. Rev. C **79**, 017302 (2009).
[29] W. N. Catford, L. K. Fifield *et al.*, Nucl. Phys. A **550**, 517 (1992).
[30] F. C. Barker, Aust. J. Phys. **40**, 25 (1987).
[31] P. Descouvemont, Phys. Rev. C **39**, 1557 (1989).
[32] P. Descouvemont, Eur. Phys. J. A **12**, 413 (2001).
[33] J. B. Marion, C. F. Cook, and T. W. Bonner, Phys. Rev. **94**, 802 (1954).
[34] Y. J. Saji, Phys. Soc. Jpn. **15**, 367 (1960).
[35] G. D. Symons and P. B. Treacy, Phys. Lett. **2**, 175 (1962).
[36] R. J. Slobodrian, H. Bichsel, J. S. C. McKee, and W. F. Tivol, Phys. Rev. Lett. **19**, 595 (1967)
[37] J. J. Kroepfl and C. P. Browne, Nucl. Phys. A **108**, 289 (1968).
[38] N. Arena, S. Cavallaro, G. Fazio, G. Giardina, A. Italiano, and F. Mezzanares, Europhys. Lett. **5**, 517 (1988).
[39] C. Scholl, Y. Fujita, T. Adachi *et al.*, Phys. Rev. C **84**, 014308 (2011).